CORTEX 67 (2015) 106–121

Available online at www.sciencedirect.com

ScienceDirect

Journal homepage: www.elsevier.com/locate/cortex

Clinical neuroanatomy

# Interhemispheric microstructural connectivity in bitemporal lobe epilepsy with hippocampal sclerosis

*Júlia Miró* [a,b], *Ane Gurtubay-Antolin* [a], *Pablo Ripollés* [a,c], *Joanna Sierpowska* [a,c], *Montse Juncadella* [b], *Lluís Fuentemilla* [a,c], *Verónica Sánchez* [d], *Mercè Falip* [b] *and Antoni Rodríguez- Fornells* [a,c,e,*]

[a] *Cognition and Brain Plasticity Group, Bellvitge Biomedical Research Institute-IDIBELL, L'Hospitalet (Barcelona), Spain*

[b] *Epilepsy Unit, Neurology Section, Hospital Universitari de Bellvitge (HUB), L'Hospitalet (Barcelona), Spain*

[c] *Department of Basic Psychology, Campus Bellvitge, University of Barcelona, L'Hospitalet (Barcelona), Spain*

[d] *Image Diagnosis Center, Hospital Clínic, Barcelona, Spain*

[e] *Catalan Institution for Research and Advanced Studies, ICREA, Barcelona, Spain*

ARTICLE INFO

*Article history:*
Received 27 October 2014
Reviewed 1 December 2014
Revised 6 February 2015
Accepted 23 March 2015
Action editor Marco Catani
Published online 1 April 2015

*Keywords:*
Commissural pathways
Diffusion tensor imaging
Mesial temporal lobe epilepsy
Interhemispheric seizure propagation
White matter

ABSTRACT

Temporal lobe epilepsy (TLE) is the most common form of focal epilepsy. The most frequent pathologic finding in this condition is hippocampal sclerosis (HS). In addition, in a small proportion (14–23%) of refractory TLE patients, the presence of HS is bilateral. TLE involves grey matter (GM) and white matter (WM) abnormalities in a wide cortico-subcortical network. However, the impact of neuronal loss on specific WM fiber pathways and associated functional systems as well as seizure propagation pathways remains unclear. There is still much controversy regarding the role of the commissures (corpus callosum, hippocampal commissure and anterior commissure) in interhemispheric seizure propagation. This study aimed to investigate the integrity of WM interhemispheric connectivity in a singular sample of patients with TLE and bilateral HS using structural magnetic resonance imaging (MRI). We performed multimodal structural MRI [high resolution T1-weighted and diffusion tensor imaging (DTI)] analyses of seven patients with medically refractory TLE with bilateral HS, fourteen unilateral left TLE patients and fifteen matched healthy individuals. Whole-brain voxel-wise analysis techniques were used. These patients evidenced WM derangement [reduced fractional anisotropy (FA), increased mean diffusivity (MD) or reduced WM volume] in temporal and extratemporal tracks, but also in commissural pathways, compared to the unilateral left TLE patients and the control group. Presence of reduced FA or increased MD in the fornix, cingulum and uncinate fasciculus in addition to reduced WM volume in the fornix was also encountered. Neuropsychological assessment was performed without significant correlations with structural data. The current results support the idea that commissural pathways play a contributory

*Abbreviations:* TLE, Temporal lobe epilepsy; HS, Hippocampal sclerosis; TLE+BHS, TLE patients with bilateral HS.

* *Corresponding author*. Cognition and Brain Plasticity Group (IDIBELL), Campus Bellvitge, Feixa Llarga, s/n (08907), L'Hospitalet de Llobregat, Spain.
E-mail address: antoni.rodriguez@icrea.cat (A. Rodríguez- Fornells).

http://dx.doi.org/10.1016/j.cortex.2015.03.018

role in interhemispheric TLE seizure propagation in bilateral HS and offer new perspectives about the long-term effects on interhemispheric connectivity associated with seizure propagation patterns in TLE patients.



## 1. Introduction

Temporal lobe epilepsy (TLE) is the most common form of focal epilepsy and also the most refractory to drug treatment (Engel, 1996). Hippocampal sclerosis (HS) represents the most frequent pathologic finding in adult patients with TLE (Malmgren & Thom, 2012). The MRI features of HS include reduced hippocampal volume, increased signal intensity on T2-weighted (or FLAIR) imaging and disturbed internal architecture (Jackson et al., 1990; Malmgren & Thom, 2012; Woermann, Barker, Birnie, Meencke, & Duncan, 1998). Interestingly, approximately 14–23% of patients with refractory TLE have the presence of bilateral HS and show independent seizure onsets from both mesial temporal regions (So, Olivier, Andermann, Gloor, & Quesney, 1989).

TLE is also the most common progressive localization-related disease (Sutula, 2004) in which the persistent paroxysmal activity during seizure alters structural and functional brain connectivity. These neuroanatomical changes can be observed in the cortex and underlying brain connectivity, having important implications not only in seizure generation and propagation but also in cognitive functioning (Marques et al., 2007; Supcun et al., 2012; Sutula, 2001). Therefore, although epilepsy is considered a grey matter (GM) disorder, pathology in patients with TLE also involves white matter (WM) abnormalities in a wide cortico-subcortical network, which is extensive and bilateral in TLE with HS (Bonilha et al., 2010; Cendes, 2005; Concha, Beaulieu, Collins, & Gross, 2009; Yogarajah & Duncan, 2008). In this vein, at the network level, the impact of TLE-related neuronal loss on specific WM fiber bundles and associated functional systems as well as seizure propagation pathways, has been largely studied (Bettus et al., 2009; Knake et al., 2009; Voets et al., 2012).

The assessment of WM pathways, particularly those through which complex partial seizures originating in temporal lobe propagate through the different ipsi- and contralateral brain structures, is an important clinical and theoretical issue, and one of particular relevance in cases in which surgical treatment might be necessary. Previous studies of TLE have extensively examined seizure propagation in the contralateral temporal lobe, although there is still much controversy regarding the matter. The most contentious point is the lack of information regarding the role of the commissures [corpus callosum, hippocampal commissure and anterior commissure] in interhemispheric seizure propagation. It has also been discussed whether these commissures permit information initially processed in the isocortex of one hemisphere to be further partially processed by the contralateral hippocampal system (Gloor, Salanova, Olivier, & Quesney, 1993; Milner, 1980). Some neurophysiological and anatomical studies (Aggleton, Desimoner, & Mishkin, 1986; Aggleton, Friedman, & Mishkin, 1987; Bertashius, 1991; Lieb, Hoque, Skomer, & Song, 1987) defend the idea that seizure transmission occurs through indirect pathways, such as the frontal lobe or subcortical structures like the mammillary bodies or midbrain reticular projections, and exclude the idea that the propagation of paroxysmal discharge is mainly due to direct or indirect commissural pathways. In contrast, more recent publications (Adam et al., 2004; Gloor et al., 1993; Spencer, Marks, Katz, Kim, & Spencer, 1992) suggest that there is evidence for a direct seizure transcommissural transfer to the contralateral temporal lobe, even though indirect non-commissural or extratemporal relays as noted above might also contribute to seizure propagation. There are also previous studies emphasizing the role of the corpus callosum as an indirect transcommissural WM route of trans-hemispheric transmission of epileptic seizure (Asadi-Pooya, Sharan, Nei, & Sperlin, 2008; Wada, 1991, 1995). In accordance with this idea, using a rat model of refractory focal neocortical epilepsy, Otte, Dijkhuizen, et al. (2012) recently showed diminished WM integrity due to seizure propagation. Strikingly, these WM abnormalities where mainly found in the corpus callosum and were not restricted to bundles close to the epileptogenic focus.

In the present study we examined GM and especially WM abnormalities in a group of TLE patients with bilateral HS (TLE+BHS), which is an uncommon subtype of focal epilepsy with bilateral disease (So et al., 1989). Where previous studies have only been devoted to TLE patients with unilateral HS (Bonilha et al., 2010; Cendes, 2005; Concha et al., 2009; Yogarajah & Duncan, 2008), this unique sample of patients with bilateral HS damage offers the opportunity to study GM and WM changes in which contralateral seizure propagation is a notable aspect of the disease (Napolitano & Orriols, 2010). To evaluate and define WM derangement we analyzed diffusion tensor imaging (DTI) images by means of tract-based spatial statistics (TBSS; Afzali, Sotlanian-Zadeh, & Elisevich, 2011; Smith et al., 2006). In addition, and as an exploratory analysis to fully characterize GM and WM abnormalities, we used voxel-based morphometry (VBM; Ashburner & Friston, 2000; Keller & Roberts, 2008) on high resolution T1-weighted images. Diffusion MRI has been described as a powerful tool for the non-invasive assessment of tissue microstructure (Concha, 2013) which has also been proved to correlate with cognitive function (Cámara, Rodríguez-Fornells, & Münte, 2010; Catani et al., 2007; López-Barroso et al., 2013). Furthermore, both VBM and TBSS are rater-independent, whole-brain voxel-wise techniques which offer a potent tool to study network atrophy without the need for defining any a priori specific brain regions.

Below, we report our findings on WM inter- and intra-hemispheric microstructural connectivity in the TLE+BHS sample, focusing on commissural pathways and their controversial role in seizure propagation. We hypothesized

that commissural pathways play a part in seizure propagation and conduction between the two anterior temporal lobes.

## 2. Methods

### 2.1. Participants

Seven patients with medically refractory TLE with Bitemporal HS (TLE+BHS; 53 ± 11 years, 4 females), fourteen patients with medically refractory left TLE (TLE+UHS; 42.93 ± 10.75 years, 10 females) and fifteen healthy individuals matched for handedness, age, gender and years of education were included in the study.

All TLE+BHS and TLE+UHS patients were recruited for a periodic clinical follow-up examination at the University Hospital of Bellvitge. Diagnosis was established according to clinical, EEG and MRI data (Cendes et al., 2000; Malmgren & Thom, 2012; Tatum, 2012; see Fig. 1). All patients underwent neurological and standardized neuropsychological examination, prolonged interictal and ictal video-EEG monitoring and structural brain MRI assessed by an expert neurologist and neuroradiologist. All of them were right-handed, as assessed with the Edinburgh handedness test (Oldfield, 1971). Patients were included in the study only if clinical data with MRI and EEG findings confirmed bilateral mesial TLE in TLE+BHS patients and left mesial TLE in TLE+UHS ones. All patients had (i) video-EEG confirming bilateral or left temporal seizure onset with typical temporal lobe EEG and semiology and (ii) moderate to severely decreased volume and abnormally increased FLAIR signal of both or left hippocampi in brain MRI. Most of the patients suffered from several comorbidities with no influence on Central Nervous System (CNS) [hypertension (2), dyslipidemia (1), heart arrhythmia (2), myopathy (1), renal disease (1)], except for two patients with depression. One of them (TLE+BHS 4) had a short evolution of a mild reactive depression and at the time of the evaluation had just started to receive psychological support instead of medical treatment. The other patient (TLE+BHS 6) had a major depressive syndrome and was under anti-depressant treatment.

The control group was composed of 15 subjects (mean age: 50 ± 13 years, 9 females). All controls were right-handed as assessed by the Edinburgh handedness test (Oldfield, 1971) and had no record of neurological illness. The study was approved by the Ethical Committee of University Hospital of Bellvitge. Informed consent was obtained from all participants. See Table 1 for demographic characteristics of the patients and control samples.

### 2.2. Neuropsychological assessment

All patients and controls completed a set of subtests from the Wechsler Memory Scale III and Wechsler Adult Intelligence Scale III (immediate and delayed verbal memory; immediate and delayed visual memory and working memory; verbal

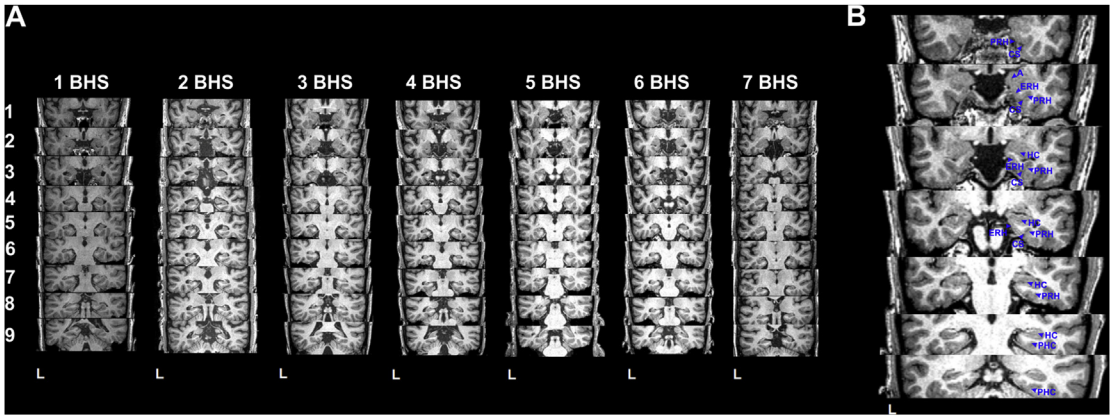


**Fig. 1 – Series of T1-weighted coronal images for each of the 7 TLE+BHS (A) and 1 representative control participant included in the study (B). (A) The sections proceed in 5 mm intervals from the perirhinal cortex in the top section caudally through the splenium of the corpus callosum in the bottom section. The top section shows the perirhinal cortex. The second section shows anterior hippocampus, the collateral sulcus and surrounding perirhinal and entorhinal cortices. The third and fourth sections show the hippocampus and the adjacent perirhinal and entorhinal cortices. Extensive hippocampal damage is evident at this level in all patients with reduced hippocampal volume of the bilateral hippocampus. Furthermore, temporal lobe atrophy and dilatation of the temporal horn accompany the hippocampal atrophy. The fifth section shows the perirhinal cortex on the lateral bank of the collateral sulcus, near the perirhinal/parahippocampal cortex border. The sixth and seventh sections show the hippocampus and the collateral sulcus, surrounded by the parahippocampal cortex. The eighth and ninth sections show the caudal border of the parahippocampal cortex, delimited by the splenium of the corpus callosum. (B) The collateral sulcus (CS) is the most important structure for the identification of medial temporal lobe cortices. At its most rostral extent, the collateral sulcus is surrounded entirely by the perirhinal cortex (PRH). Caudally, the entorhinal cortex (ERH) extends from the midpoint of the medial bank of the collateral sulcus to the subiculum, whereas the perirhinal cortex extends laterally from the midpoint of the medial bank of the collateral sulcus to the inferotemporal cortex. Two millimeters caudal to the disappearance of the gyrus intralimbicus of the hippocampus (HC), the collateral sulcus is surrounded by the parahippocampal cortex (PHC). L: left hemisphere.**

**Table 1 – Demographic characteristics of patient and control samples.**

| | Gender | Age (Y) | Onset (Y) | Duration (Y) | MRI | Frequency | Num. AEDs | IPI |
|---|---|---|---|---|---|---|---|---|
| TLE+BHS 1 | F | 55 | 45 | 10 | BHS | 15–20 | 2 | Yes |
| TLE+BHS 2 | M | 64 | 7 | 57 | BHS | 3–4 | 3 | Yes |
| TLE+BHS 3 | M | 56 | 14 | 42 | BHS | 1–2 | 2 | Yes |
| TLE+BHS 4 | F | 43 | 12 | 31 | BHS | 10–16 | 2 | Yes |
| TLE+BHS 5 | M | 53 | 3 | 50 | BHS | 1 | 2 | No |
| TLE+BHS 6 | F | 35 | 3 | 32 | BHS | 8–16 | 2 | Yes |
| TLE+BHS 7 | F | 65 | 12 | 53 | BHS | 1–2 | 2 | NK |
| TLE+UHS 1 | F | 37 | 1 | 36 | LHS | 3–4 | 2 | No |
| TLE+UHS 2 | F | 62 | 3 | 59 | LHS | 4 | 2 | No |
| TLE+UHS 3 | F | 34 | 16 | 18 | LHS | 15–20 | 3 | Yes |
| TLE+UHS 4 | M | 38 | 5 | 33 | LHS | 4–5 | 3 | Yes |
| TLE+UHS 5 | F | 49 | 1 | 48 | LHS | 4–5 | 2 | Yes |
| TLE+UHS 6 | F | 40 | 1 | 39 | LHS | 5–6 | 4 | Yes |
| TLE+UHS 7 | F | 44 | 40 | 4 | LHS | 1–2 | 2 | Yes |
| TLE+UHS 8 | M | 29 | 15 | 14 | LHS | 3–4 | 3 | No |
| TLE+UHS 9 | M | 25 | 14 | 9 | LHS | 1–2 | 2 | Yes |
| TLE+UHS 10 | F | 50 | 32 | 18 | LHS | 18–20 | 2 | No |
| TLE+UHS 11 | F | 46 | 8 | 38 | LHS | 13–15 | 3 | Yes |
| TLE+UHS 12 | F | 35 | 2 | 33 | LHS | 4–6 | 2 | No |
| TLE+UHS 13 | F | 58 | 10 | 48 | LHS | 3–4 | 2 | Yes |
| TLE+UHS 14 | M | 53 | 15 | 38 | LHS | 2–3 | 2 | No |
| Controls | 9F | 50 (13) | – | – | Normal | – | – | – |

For controls, the data represent the mean followed by the standard deviation in parenthesis. Seizure frequency refers to the number of self-reported complex-partial seizures (CPS) per month. F, female; M, male; Y: years; BHS: bilateral hippocampal sclerosis; LHS: left hippocampal sclerosis; Num. AEDs: Number of Antiepileptic Drugs; IPI: initial precipitant incident. NK: not known.

comprehension and perceptual organization; Wechsler, 1997, 2004).

The Boston Naming Test (Kaplan, Goodglass, & Weintraub, 1983), Semantic and Phonological fluency tests (Peña-Casanova, 2005) and the Trail Making Test (Reitan, 1992) were also carried out by all participants in order to explore naming abilities, verbal fluency and processing speed, respectively (see Table 2). All these scores were compared to normative data, minimizing the possible bias of age and education in further statistical analysis. The Rey Auditory Verbal Learning test (RAVLT) was also performed, measuring the learning capability (total amount of correct responses) and delayed retrieval and recognition of the word list (results of RAVLT measures are all reported as a raw score due to a lack of normative data for the Spanish population).

In order to detect possible differences between groups, statistical analyses were performed with PASW Statistics v18.0 (SPSS Inc. Chicago, IL, USA). At the group level, a two-sample Student *t*-test was employed for each of the neuropsychological subtests. The statistical significance threshold was set at $p < .05$. Further, similarly to the analysis of the neuroimaging data (see below), the patients' neuropsychological performance was investigated using a single case study approach. Each patient's results were analyzed by means of a modified *t*-test developed for use in clinical practice and single case research (Crawford & Howell, 1998). This method allowed a comparison between an individual patient's test score and norms derived from the control sample. Bearing in mind that in TLE the pathology and severity may vary, this additional analysis allowed better characterization of the level of cognitive impairment of each patient separately on each task (for more details see, Towgood, Meuwese, Gilbert, Turner, & Burgess, 2009).

### 2.3. *Image acquisition*

Controls, TLE+UHS and TLE+BHS patients underwent whole-brain structural MRI scans using a 3.0 Tesla Siemens Trio MRI at the Hospital Clinic of Barcelona. A 32-channel phased-array head coil system was used to acquire high resolution T1-weighted images (slice thickness = 1 mm; no gap; number of slices = 240; TR = 2300 msec; TE = 3 msec; matrix = 256 × 256; FOV = 244 mm; voxel size = 1 × 1 × 1 mm), and a DTI sequence was carried out using diffusion tensor spin-echo planar imaging with coverage of the whole head (voxel size of 2.5 × 2.5 × 2.5 mm, matrix of 96 × 96, 55 slices with 2.5 mm-thick and no gap, TE = 98 msec, TR = 9600 msec, EPI factor = 96, field of view = 240 mm, bandwidth = 1022 Hz, echo-spacing = 1.08 msec, b-value = 1000 sec/mm$^2$). For the DTI data, one single run of 64 diffusion-weighted directions with one non-diffusion-weighted volume was acquired. In addition, for diagnostic purposes only, TLE+UHS and TLE+BHS patients were also scanned on a 1.5 Philips Intera scan at the University Hospital of Bellvitge to acquire an FLAIR image (slice thickness = 5.2 mm; no gap; number of slices = 19; TR = 7295 msec; TE = 12 msec; matrix = 256 × 256; FOV = 230 mm; voxel size = .89 × 0.89 × 5.2 mm). Both structural scans (T1 and FLAIR) were assessed by two experienced neurologists and one neuroradiologist who found no structural abnormalities besides HS bilaterally in TLE+BHS patients and left in TLE+UHS ones.

### 2.4. *Image processing*

#### 2.4.1. *T1-weighted processing*

First, an exploratory analysis with the aim of confirming GM abnormalities and to initially explore WM damage in the

**Table 2 – Neuropsychological results of TLE+BHS patients and control samples reported at the group level.**

| MEASURE | TLE+BHS (n=7) | CONTROLS (n=15) | p |
|---|---|---|---|
| *Age* | 53±10.82 | 47.87±10.48 | 0.30 |
| *Sex* | 1.57±0.53 | 1.67±0.49 | 0.68 |
| *Years of education* | 9.86±2.73 | 11.40±2.97 | 0.25 |
| *Handedness* | 1.57±1.51 | 1.54±1.09 | 0.96 |
| *Immediate verbal memory* | 6.14±2.41 | 5.93±1.83 | 0.82 |
| *Delayed verbal memory* | 5.43±2.76 | 9.20±2.34 | 0.003 |
| *Immediate visual memory* | 6.29±2.98 | 10.93±2.87 | 0.002 |
| *Delayed visual memory* | 5.14±2.67 | 9.47±2.07 | **0.001** |
| *Visual recognition* | 4.8±1.9 | 9.4±2.4 | 0.002 |
| *WM: Digit Span* | 9.00±3.1 | 8.87±2.59 | 0.92 |
| *WM: L & N* | 7.14±3.02 | 9.20±3.07 | 0.16 |
| *VC: Vocabulary* | 8.86±2.67 | 11.53±2.03 | 0.01 |
| *VC: Similiarities* | 9.33±1.97 | 11.27±3.17 | 0.11 |
| *PC: Block design* | 8.33±2.16 | 9.47±3.02 | 0.35 |
| *BNT* | 7±2.58 | 10.13±2.64 | 0.01 |
| *Fluency (Phonological - "p")* | 7.86±5.46 | 10.47±1.99 | 0.26 |
| *Fluency (Semantic-animals)* | 6.14±3.13 | 9.40±2.50 | 0.01 |
| *TMTA* | 6.00±3.22 | 9.93±3.61 | 0.03 |
| *TMTB* | 7.1±3.43 | 8.53±3.34 | 0.43 |
| *RAVLT total score* | 34.71±9.65 | 44.60±8.89 | 0.02 |
| *RAVLT Delayed word list retrieval* | 4.7±2.4 | 8.3±2.8 | 0.008 |
| *RAVLT Delayed word list recognition* | 12.0±3.2 | 13.8±1.3 | 0.2 |

p >0.05; p <0.05; p <0.01; **p <0.001**

The comparison between the overall neuropsychological performance of TLE+BHS patients versus controls is represented with the mean and standard deviation of the normalized tests scores (normalization according to age and educational level in all tests, except Rey Auditory Learning Test; for the normative data see Methods section). Handedness: 1 = Right and 5 = Left; WM: working memory; L & N: Letters and Numbers; VC: Verbal Comprehension; PC: perceptual organization; BNT: Boston Naming Test; TMT: Trail Making Test; RAVLT: Rey Auditory Verbal Learning test.

TLE+BHS group was carried out using Voxel-Based Morphometry (VBM; Ashburner & Friston, 2000) under Statistical Parametric Mapping software (SPM8; Wellcome Department of Imaging Neuroscience, University College, London, UK, www.fil.ion.ucl.ac.uk/spm) and MATLAB 7.8.0 (The MathWorks Inc, Natick, Mass). Specifically, New Segment, an improved version of Unified Segmentation (Ashburner & Friston, 2005), was applied to the structural T1-weighted images of each subject in the control and TLE+BHS groups. The resulting tissue probability maps (GM and WM) were imported and fed into Diffeomorphic Anatomical Registration using Exponentiated Lie algebra (DARTEL; Ashburner, 2007) to achieve spatial normalization in Montreal Neurologic Institute (MNI) space (Ripollés et al., 2012). The group-specific template created by DARTEL included all subjects from the control and TLE+BHS groups. DARTEL normalization alternates between computing an average template of the GM and WM segmentations from all subjects and warping all subjects' GM and WM

segmentations into better alignment with the template created (Ashburner & Friston, 2009). Normalized images were smoothed using an isotropic spatial filter (FWHN = 6 mm) to reduce residual inter-individual variability.

All normalized and smoothed GM and WM images from healthy subjects and the TLE+BHS group were further analyzed in order to compare GM and WM volumetrically (using "modulation" to compensate for the effect of spatial normalisation, Mechelli, Price, Friston, & Ashburner, 2005). The individual smoothed GM and WM volume images were entered into a second-level analysis using a two-sample Student t-test (Healthy > TLE+BHS) employing a random effects analysis within the general linear model. A mask, covering all brain tissue, was used to restrict the analyses, as we were also interested in detecting differences in GM and WM boundaries. Results are reported at an uncorrected $p < .005$ threshold, and areas surviving a $p < .05$ FWE-correction at the cluster level are indicated with an asterisk in Table A.1.

#### 2.4.2. *DTI processing*

DTI raw data was first motion and eddy-current corrected, using Functional Magnetic Resonance Imaging of the Brains' (FMRIB's) Diffusion Toolbox (FDT), part of the Functional Magnetic Resonance Imaging of the Brain Software Library (FSL www.fmrib.ox.ac.uk/fsl/; Smith et al., 2004; Woolrich et al., 2009). The gradient matrix was then rotated and the structural image was fully-stripped using Functional Magnetic Resonance Imaging of the Brain Software Library's (FSL's) Brain Extraction Tool (Smith et al., 2002). Diffusion tensors were reconstructed using the linear least-squares method provided in Diffusion Toolkit (Ruopeng Wang, Van J. Wedeen, TrackVis.org, Martinos Center for Biomedical Imaging, Massachusetts General Hospital). The tensor was spectrally decomposed in order to obtain its eigenvalues and eigenvectors. The fiber direction was assumed to correspond to the principal eigenvector (the eigenvector with the largest eigenvalue). Fractional anisotropy (FA), axial diffusivity (AD), radial diffusivity (RD) and mean diffusivity (MD)/apparent diffusion coefficient (ADC) values were generated from these eigenvalues. FA quantifies the anisotropy in each voxel, with values ranging from 0 (fully isotropic) to 1 (diffusion is favored in one axis and hindered in the remaining two). AD represents the diffusiveness value along the main axis direction. RD is calculated as the mean of the remaining two directions. Finally, MD or ADC is a scalar measure reflecting the total diffusion within a voxel which is equivalent to the average of the eigenvalues. In degenerated tracts, water diffusion is more isotropic; thus FA and AD are expected to decrease, while MD and RD are expected to increase (Beaulieu, 2002; Song et al., 2002).

In order to compare patient FA, AD, RD and MD values to those of the control group in a voxel-wise manner, we used Functional Magnetic Resonance Imaging of the Brain Software Library's Tract-Based Spatial Statistics (TBSS; Smith et al., 2006). FA maps from all participants (controls, TLE+UHS and TLE+BHS) were registered to a Montreal Neurologic Institute FA template (FMRIB58_FA, MNI152 space) using Functional Magnetic Resonance Imaging of the Brain's Nonlinear Image Registration Tool (FNIRT; Andersson, Jenkinson, & Smith, 2007a; 2007b). All registrations were then visually inspected and no noticeable misalignment was detected. A mean FA volume was first created (thresholded at FA > .2) and then used to generate an FA skeleton that corresponded to the center of the major WM tracts in the brain. Each participant's normalized FA data were projected onto this skeleton by searching for the highest FA value within a search space perpendicular to each voxel of the mean skeleton. This process was repeated for the RD, AD and MD maps by applying the transformations previously calculated for the FA maps. The resulting data were fed into voxel-wise cross-subject statistics (Smith et al., 2006).

In order to achieve accurate statistical inference, including appropriate correction for multiple comparisons, we used permutation-based non-parametric testing on a voxel-by-voxel basis (Nichols & Holmes, 2002). A two-sample t-test (5000 permutations) was used to assess the location and extent of significant increases and decreases in FA, AD, RD and MD maps between TLE+BHS and TLE+UHS patients and between TLE+BHS patients and the control group. Threshold-free cluster enhancement (Smith & Nichols, 2009) was used to correct results for multiple comparisons using a Family Wise Error (FWE) corrected $p < .05$ threshold.

Significant clusters were superimposed onto the Montreal Neurologic Institute FA template (MNI152) supplied in FSL.In FSL view and its atlas tools (International Consortium of Brain Mapping DTI-81 WM labels atlas and John Hopkins University WM probabilistic tractography atlas), in addition to general neuroanatomy atlases (Catani & Thiebaut de Schotten, 2012; Mori, Faria, Oishi, & van Zijl, 2005), were used to anatomically label the location of significant clusters in MNI152 space.

An additional exploratory analysis was carried out as a means to assess each patient's damage separately. Thus, each patient's whole-brain FA skeleton was compared to those of the control group through a modified version of the independent samples t-test, which accounts for the limited size of the control group ($p = .05$; Crawford & Garthwaite, 2004; Crawford & Howell, 1998). This method has previously been used to compare a stroke patient with a control group using the TBSS approach (Tuomiranta et al., 2014).

## 3. Results

### 3.1. *Demographic and neuropsychological data*

Table 1 shows demographic characteristics for the TLE+BHS and TLE+UHS patients and the control group (see Fig. 1 for anatomical images of all TLE+BHS patients and one reference control subject). Table 2 shows neuropsychological performance of TLE+BHS patients and controls recruited for this study. We found no statistically significant differences in age, sex, years of education or handedness between TLE+BHS patients and healthy subjects (n.s., all $p > .05$). At the group level, the TLE+BHS patients scored significantly lower than controls in several memory scales such as immediate visual memory, delayed visual memory and delayed verbal memory ($p < .01$). Furthermore, we found a similar pattern in TLE+BHS patients in speech processing assessments. TLE+BHS patients appeared to be significantly impaired ($p < .01$) in the Boston Naming Test, Semantic Fluency tests, vocabulary comprehension (WAIS III) and the Rey Auditory Verbal Learning Test

when compared with the control group (for references see methods; for results see Table 2). Patients' processing speed abilities were also affected, as measured with the executive measure of the Trail Making Test ($p < .05$).

At the single case analysis level, the results confirmed that patients and healthy controls differed the most in memory performance (mainly at the RAVLT delayed word list retrieval; for more details on the individual differences in the neuropsychological tests scores, please consult Table 3.).

### 3.2. VBM results for WM and GM

Voxel-wise analysis of the T1-weighted images revealed widespread damage, albeit slightly left predominant, with WM and GM reductions in TLE+BHS patients compared to controls (see Table A.1 and Figure A.1). As expected, significant WM reduction was found bilaterally at the parahippocampal gyrus, at the fornix (temporal fibers, fimbria, body and posterior columns), and also at the hippocampal commissure (small posterior component of the fornix fimbria; green regions in Fig. A.1A). There was also a significant reduction in GM that affected the left hippocampus, thalamus and parahippocampal area (red regions in Fig. A.1A). A significant overlap between clusters of WM and GM in the left hippocampus and parahippocampal gyrus was clearly observed (see Fig. A.1B).

### 3.3. TBSS results

Several WM pathways with decreased FA were detected in TLE+BHS patients compared with controls (see Table 4, Fig. 2 and Fig. A.1C). Interestingly, the extent of FA reduction was more prominent overall in the left than in the right hemisphere (see Fig. 2). Many limbic pathways (connecting inter and intrahemispherical brain regions) also showed significantly decreased FA (i.e., bilateral fornix, internal capsule, cingulum, uncinate fasciculus and the anterior commissure).

**Table 3 – Single case study results for the neuropsychological tests of TLE+BHS patients compared to the control sample.**

| *MEASURE* | P1 | P2 | P3 | P4 | P5 | P6 | P7 |
|---|---|---|---|---|---|---|---|
| *Immediate verbal memory* | 0,04 | 1,62 | -0,49 | 0,04 | 1,62 | *-2,08* | 0,04 |
| *Delayed verbal memory* | *-2,16* | -1,74 | -1,74 | -0,91 | 0,33 | -3,40 | -1,33 |
| *Immediate visual memory* | *-2,01* | -0,65 | *-2,01* | *-2,01* | 0,02 | -3,02 | -1,33 |
| *Delayed visual memory* | *-2,56* | *-2,09* | -3,03 | -1,16 | -0,69 | -3,97 | -0,69 |
| *Visual recognition* | *-2,54* | *-2,14* | *-2,14* | - | -0,55 | - | -1,74 |
| *WM: Digit Span* | -0,70 | 1,17 | 0,80 | 0,42 | 0,80 | *-2,20* | 0,05 |
| *WM: L & N* | -1,64 | 0,25 | 0,57 | -0,06 | -0,69 | *-1,95* | -1,01 |
| *VC: Vocabulary* | -1,21 | -0,25 | -0,73 | 0,22 | -1,21 | -3,59 | *-2,16* |
| *VC: Similiarities* | -0,39 | -0,08 | -0,08 | -1,00 | -0,39 | - | -1,61 |
| *PC: Block design* | -0,79 | 0,17 | -0,15 | -1,43 | 0,49 | - | -0,47 |
| *BNT* | -1,15 | -0,05 | -0,42 | -1,15 | -1,51 | -2,98 | -0,78 |
| *Fluency (Semantic-animals)* | -1,70 | 1,01 | -0,93 | -0,93 | -1,32 | -2,86 | *-2,09* |
| *Fluency (Phonological - "p")* | 1,23 | *2,20* | 0,74 | -1,68 | -3,14 | **-4,11** | **-4,11** |
| *TMTA* | -1,05 | 0,29 | *-1,86* | -0,79 | -0,79 | - | *-2,13* |
| *TMTB* | -0,74 | 0,43 | 0,14 | -1,03 | 0,72 | - | *-1,90* |
| *RAVLT total score* | -0,07 | -0,17 | -0,17 | -1,26 | -0,94 | -2,68 | *-2,24* |
| *RAVLT Delayed word list retrieval* | **-5,21** | **-4,44** | **-7,50** | **-7,50** | **-5,97** | **-8,27** | **-9,80** |
| *RAVLT Delayed word list recognition* | *-0,46* | *-0,11* | -1,49 | -1,49 | *-0,80* | -1,83 | -2,52 |

p >0.05; p <0.05; p <0.01; **p <0.001**; '-', missing data

The comparison between the normalized tests scores of each TLE+BHS patient on each task separately versus their corresponding control group ($n = 15$, normalization according to age and educational level in all tests, except RAVLT; for the normative data see Methods section). The results are represented with the t-value and marked according to their significance level. P, Patient; WM: working memory; L & N: Letters and Numbers; VC: verbal comprehension; PC: perceptual organization; BNT: Boston Naming Test.

**Table 4 – TBSS analysis: representative pathways in the whole-brain analysis for the FA maps for the control > TLE+BHS patient contrast (tracts showing less FA in patients than in controls), with their respective *p*-values ($p < .05$ Family Wise Error-corrected) and MNI coordinates.**

| White Matter tract | Hemisphere | *p* value | Peak MNI coordinates | | |
|---|---|---|---|---|---|
| | | | *x* | *y* | *z* |
| SCR | L | .0182 | −26 | 5 | 29 |
| SLF | L | .0192 | −36 | 11 | 19 |
| IC-ATR | L | .0198 | −21 | 13 | 16 |
| SCC | Inter | .0218 | −1 | −35 | 18 |
| BCC | R | .0218 | 7 | −26 | 24 |
| BCC | L | .0218 | 0 | −29 | 21 |
| GCC | Inter | .0230 | −1 | 25 | 11 |
| GCC | L | .0230 | −11 | 25 | 18 |
| SCC | L | .0230 | −13 | −31 | 27 |
| EC-Unc | L | .0230 | −22 | 18 | −10 |
| EC-IFOF | L | .0230 | −35 | −12 | −11 |
| Cing | L | .0232 | −11 | −32 | 31 |
| Fx | L | .0232 | −30 | −19 | −8 |
| ILF | L | .0238 | −43 | −28 | −6 |
| Fmi | L | .0244 | −15 | 41 | −12 |
| IFOF | L | .0244 | −37 | −14 | −12 |
| Cing | R | .0250 | 9 | 18 | 28 |
| AC | L | .0298 | −18 | −3 | −9 |
| IC-ATR | R | .0316 | 21 | 13 | 11 |
| IFOF | R | .0330 | 27 | 33 | 8 |
| Unc | R | .0336 | 15 | 37 | −12 |
| Fmi | R | .0336 | 18 | 39 | −2 |
| GCC | R | .0338 | −14 | 26 | 18 |
| SCP | R | .0360 | 2 | −22 | −12 |
| Fx | R | .0432 | 31 | −21 | −8 |
| EC-Unc | R | .0444 | 34 | 2 | −10 |
| SLF | R | .0450 | 44 | −41 | −3 |
| AC | R | .0472 | 10 | −3 | −5 |
| ILF | R | .0490 | 51 | −3 | −9 |
| SCC | R | .0494 | 13 | −34 | 25 |

Coordinates are given following the Montreal Neurologic Institute system. AC: anterior commissure; ATR: anterior thalamic radiation; BCC: body of corpus callosum; Cing: cingulum; EC: external capsule; Fma: forceps major; Fmi: forceps minor; Fx: fornix; IC: internal capsule; GCC: genu corpus callosum; IFOF: inferior fronto-occipital fasciculus; ILF: inferior longitudinal fasciculus; SCC: splenium corpus callosum; SCP: superior cerebellar peduncle; SCR: superior corona radiata; SLF: superior longitudinal fasciculus; Unc: uncinate. L: left hemisphere; R: right hemisphere.

In addition, other major extralimbic WM tracts such as the corpus callosum (the great white commissure that crosses the longitudinal cerebral fissure and interconnects the hemispheres) showed reduced FA values throughout its entire route, with the lowest values in the genu and body in TLE+BHS patients compared to control participants. The most significant overlap of WM loss between VBM and TBSS studies was observed in the fornix (Fig. A.1C).

Furthermore, increased MD in TLE+BHS patients compared to controls was observed in interhemispheric pathways of the body and genu of corpus callosum in TLE+BHS patients (see Fig. 2 and Table 5). Limbic pathways (e.g., fornix, internal capsule and uncinate fasciculus) and other extralimbic WM tracts anatomically close to the hippocampus such as inferior longitudinal fasciculus and inferior fronto-occipital fasciculus were also found to have increased MD. Increases in MD in the anterior regions of the brain appeared to be statistically more significant than in the posterior regions (see Fig. 2). No difference was found for RD, but decreased AD in the body of the corpus callosum was found to be marginally significant ($p = .06$). In line with these results, quantitative FA and MD values in interhemispheric pathways showed reduced FA in TLE+BHS patients in the anterior commissure and in the corpus callosum.

The overlap between increased MD and decreased FA in patients compared to controls comprised several interhemispheric (genu and body of the corpus callosum) and intrahemispheric limbic (fornix or uncinate fasciculus) WM pathways, in addition to intrahemispheric extralimbic bundles such as the superior and inferior longitudinal fasciculus and inferior fronto-occipital fasciculus (see Fig. 2).

The analysis comparing each TLE+BHS patient's FA map to the control group revealed high inter-subject variability. However, all patients showed FA decreases when compared to the control group in several common pathways, the most prominent being the largest commissural bundle: the corpus callosum (mainly genu and body; see Fig. 3). Specifically in TLE+BHS 1 and TLE+BHS 3 patients who showed the most severe abnormalities, decreased FA was found in the genu and the body of the corpus callosum (supplementary to the splenium of the corpus callosum in TLE+BHS 1), in addition to severe bilateral damage adjacent to both hippocampi. Furthermore, inferior longitudinal and inferior fronto-occipital fascicles were also found to be bilaterally damaged in both of patients. Bilateral superior longitudinal fascicles appeared to be deteriorated bilaterally in TLE+BHS 1, in contrast to TLE+BHS 3, who only showed left superior longitudinal fasciculus damage.

Finally, for the comparison between TLE+BHS and TLE+UHS patients, MD increases were found in the TLE+BHS group only. In line with previous results, the extent of MD increase was more prominent in the left hemisphere (see Fig. 4 and Table 6). Particularly, the genu and body of the corpus callosum in the left hemisphere were found to be the most affected areas in addition to other interhemispheric pathways such as the right corpus callosum and the fornix (right and left hemispheres). Other limbic tracts (cingulum, internal capsule or uncinate fasciculus) also showed MD increment.

## 4. Discussion

This study evaluated, for first time to our knowledge, WM inter- and intrahemispheric microstructural connectivity in a cohort of patients with medically refractory TLE and Bitemporal HS (TLE+BHS). This singular and uncommon patient group (So et al., 1989) offered the opportunity to study interhemispheric connectivity in a sample of patients in which hemispheric transmission plays a notable role (Napolitano & Orriols, 2010). Moreover, the use of multimodal imaging (T1-weighted and DTI images) and whole-brain voxel-wise analysis techniques (VBM and TBSS) allowed us to detect a pattern of WM abnormalities that goes beyond the focal nature of TLE (Afzali et al., 2011; Gross, 2011; Keller and Roberts., 2008). As

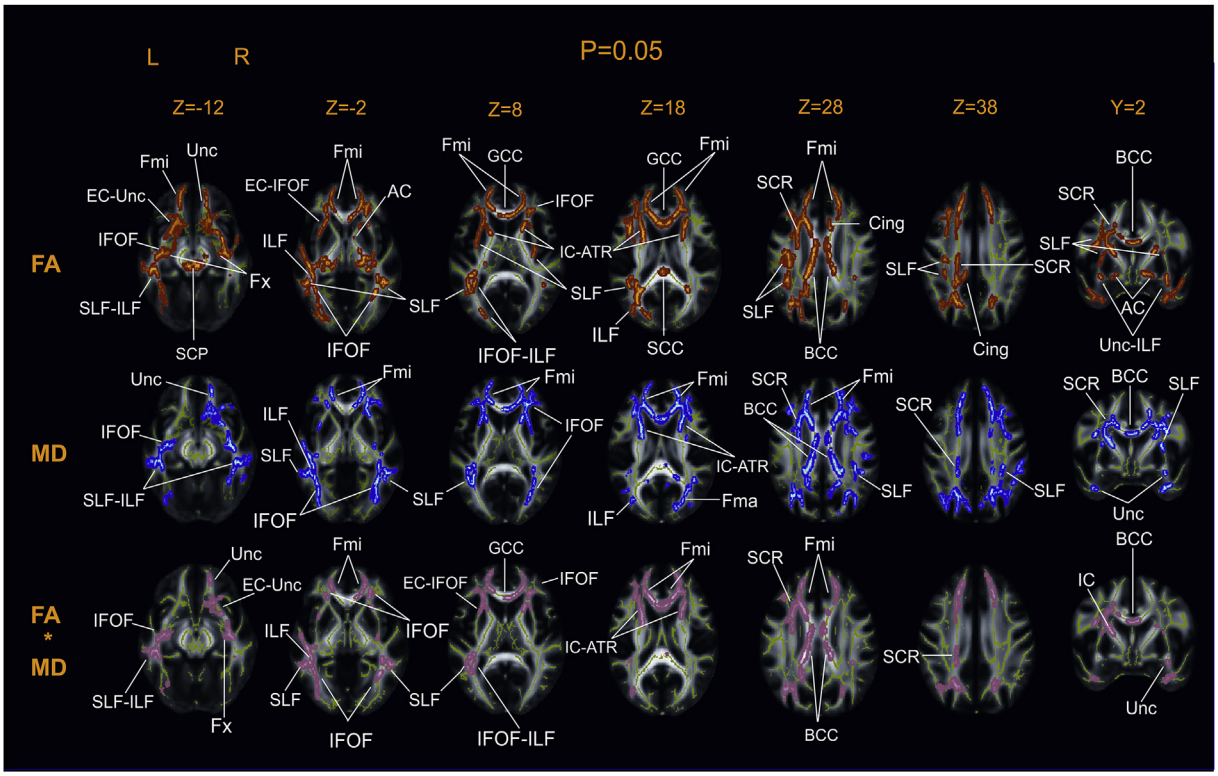


**Fig. 2 – Significant clusters of decreased FA and increased MD in TLE+BHS patients found with TBSS analysis when compared with controls. Results are shown at a Family Wise Error-corrected $p < .05$ threshold. Significant clusters representing decreases in FA in the TLE+BHS group compared with controls are shown in the upper row (red to yellow), increases in MD are shown in the middle row (light to dark blue) and overlap of FA decreases and MD increases are shown in the bottom row (purple). All clusters are projected onto a Montreal Neurological Institute FA template (FMRIB58_FA, MNI152 space) provided by FSL, and the mean group FA skeleton is shown in green. AC: anterior commissure; ATR: anterior thalamic radiation; BCC: Body of corpus callosum; Cing: cingulum; EC: external capsule; Fma: forceps major; Fmi: forceps minor; Fx: fornix; IC: internal capsule; GCC: genu corpus callosum; IFOF: inferior fronto-occipital fasciculus; ILF: inferior longitudinal fasciculus; SCC: splenium corpus callosum; SCP: superior cerebellar peduncle; SCR: superior corona radiata; SLF: superior longitudinal fasciculus; Unc: uncinate. L: left hemisphere; R: right hemisphere.**

expected, during neuropsychological assessment, the TLE+BHS patient group scored significantly lower in several memory scales such as immediate visual memory, delayed visual memory and verbal memory (Hoppe, Elger, & Helmstaedter, 2007). These results were confirmed as well by the single case analysis (illustrating especially RAVLT delayed word list retrieval problems). The multimodal imaging results showed WM derangement (reduced FA, increased MD or reduced WM volume) in commissural pathways (the corpus callosum, the anterior commissure or the hippocampal commissure) in TLE+BHS patients when compared to unilateral left TLE patients and to a healthy matched control group. Furthermore, presence of extended and significant WM abnormalities in limbic (reduced FA or increased MD in the fornix, cingulum or uncinate fasciculus and also reduced WM volume in the fornix) but also in extralimbic structures (reduced FA or increased MD in the inferior longitudinal fasciculus and inferior fronto-occipital fasciculus) was found. The present results also indicated that the most affected areas in bilateral patients when compared to unilateral TLE patients (TLE+UHS) were the genu and body of the corpus callosum. As expected, GM atrophy in TLE+BHS patients was also found in the hippocampus (see Table A.1 and Figure A.1). Interestingly, all these structural and connectivity abnormalities, although bilateral, were more significant in the left hemisphere.

The knowledge of anatomical connections of WM fibers linking the hippocampus as part of the inter- and intrahemispheric neural network of TLE is essential for a deeper understanding of the network involved in the generation, propagation and maintenance of seizures. Regarding interhemispheric tracts, a significant FA decrease and MD increase was detected in the body and the genu of the corpus callosum compared with the control group, and an MD increase compared with unilateral left TLE patients. These findings support previous studies emphasizing the role of the corpus callosum as an indirect WM route of trans-hemispheric transmission in epileptic seizure (Asadi-Pooya et al., 2008; Otte et al., 2012; Wada, 1991, 1995). In the case of seizure

**Table 5 – TBSS analysis: representative pathways in the whole-brain analysis of the MD maps for the TLE+BHS patients > controls contrast (patients with higher MD than controls), with their respective *p*-values ($p < .05$ Family Wise Error – corrected) and MNI coordinates.**

| White Matter tract | Hemisphere | *p* value | Peak MNI coordinates | | |
|---|---|---|---|---|---|
| | | | x | y | z |
| ACR-IFOF | R | .0152 | 25 | 30 | −1 |
| Fmi | R | .156 | 18 | 38 | 5 |
| BCC | R | .0174 | 16 | 15 | 29 |
| IC-ATR | R | .0178 | 20 | 15 | 8 |
| GCC | R | .0190 | 13 | 31 | 10 |
| EC-IFOF | R | .0202 | 28 | 19 | 1 |
| GCC | Inter | .0156 | 0 | 25 | 11 |
| ACR-ATR | L | .0244 | −21 | 24 | 25 |
| BCC-GCC | L | .0256 | −14 | 19 | 25 |
| BCC | Inter | .0262 | 0 | −3 | 25 |
| Fmi | L | .0296 | −17 | 38 | 6 |
| EC-Unc | R | .0296 | 24 | 20 | −9 |
| SLF | L | .0310 | −33 | 6 | 25 |
| SCC | R | .0324 | 19 | −42 | 27 |
| SCR | L | .0334 | −26 | −7 | 25 |
| ILF | L | .0354 | −44 | −33 | −9 |
| EC | L | .0360 | −28 | 8 | 12 |
| SCC | L | .0408 | −18 | −38 | 29 |
| Fx | L | .0426 | −31 | −13 | −12 |
| SLF | R | .0474 | 39 | −45 | 23 |

Coordinates are given following the Montreal Neurologic Institute system. WM: white matter; ACR: anterior corona radiata; ATR: anterior thalamic radiation; BCC: body of corpus callosum; Cing: cingulum; EC: external Capsule; Fmi: forceps minor; Fx: fornix; GCC: genu corpus callosum; IC: internal capsule; IFOF: inferior fronto-occipital fasciculus; ILF: inferior longitudinal fasciculus; SCC: splenium corpus callosum; SCP: superior cerebellar peduncle; SCR: superior corona radiata; SLF: superior longitudinal fasciculus; Unc: uncinate. L, left hemisphere; R, right hemisphere.

originating in the temporal lobe, the anterior half (genu and body) of the corpus callosum is probably the most important route as its trans-hemispheric transmission may use a temporal ipsilateral frontal pathway through the corpus callosum to the contralateral frontal hemisphere and then on to the contralateral temporal limbic system (Wada, 1991, 1995). However, depth electrode EEG recordings of temporal lobe seizures have also shown, in some instances, a pattern of contralateral spread that is consistent with a direct commissural propagation via the anterior or dorsal hippocampal commissure. In these cases, hippocampal seizure discharges have been observed to spread to the contralateral hippocampus before the contralateral neocortex is involved in the ictal discharge, highlighting their role in interhemispheric seizure propagation (Adam et al., 2004; Gloor et al., 1993; Spencer et al., 1992). In accordance with this, our TLE+BHS patients compared with the control group showed a significant FA decrease in interhemispheric connectivity fibers such as the anterior commissure, which is located in front of the columns of the fornix and also assumes the role of a direct connection for both anterior temporal lobes (Di Virgilio, Clarke, Pizzolato, & Schaffner, 1999). Unilateral TLE differences have been detected in the fornix in previous studies (Concha et al., 2009; Concha, Beaulieu, & Gross, 2005; Concha, Livy, Beaulieu, Whatley, & Gross, 2010), though not specifically in the hippocampal commissure or commissure of the fornix. Although FA decreases in the corpus callosum have also been reported in unilateral TLE WM studies (Arfanakis et al., 2002; Concha et al., 2009; Gross, Concha, & Beaulieu, 2006; Keller, Schoene-Bake, Gerdes, Weber, & Deppe, 2012), our results show, for the first time to our knowledge, that TLE patients with BHS have an increase in MD (see Fig. 4) in the fibers of the corpus callosum compared to unilateral TLE patients with left HS. In addition, another exploratory finding when comparing TLE+BHS patients with controls was WM abnormalities (less WM volume in the VBM analysis) found bilaterally in the hippocampal commissure, which crosses the midline to project directly to the contralateral parahippocampal gyrus and hippocampus.

Concurrent with the well-recognized relevance of the limbic system as a key part of the neural circuitry of TLE (Kuzniecky et al., 1999), we found decreased FA in bilateral fornix and cingulum (the most prominent WM tracts within the limbic system) and also in the uncinate fasciculus when comparing TLE+BHS patients to both healthy controls and unilateral TLE patients (see Figs. 2 and 4). In the fornix we even found an increase in MD/decrease in FA which may be related to the WM volume decrease also found in that structure (especially with partial voluming of the tissue surrounding the fornix) in the healthy control group comparison (see Fig. A.1C). The WM abnormalities seen bilaterally in the fornix, the cingulum and the uncinate fasciculus are also in accordance with previous studies (Concha et al., 2005, 2009, 2010; Diehl et al., 2008). Interestingly, the results in TLE with bilateral HS shown here regarding the fornix concur with a recent study combining DTI and histological analysis of resected fimbria-fornix in unilateral temporal lobe epilepsy patients (Concha, Livy, Beaulieu, Whatley, & Gross, 2010). In this study, patients with HS and reduced FA in the fimbria-fornix showed larger extra-axonal spaces, less myelin fraction and a decreased number of axons in the resected fimbria-fornix tissue in the histological analysis. Importantly, FA values in this region correlated with the surface area of axonal membranes and also marginally with axonal density (Concha et al., 2010). Similar results have been observed in a postmortem study of TLE (with HS) patients, in which decreased axonal density of the fimbria-fornix was observed bilaterally (Ozdogmus, Cavdar, Ersoy, Ercan, & Uzun, 2009). Nevertheless, findings regarding the contralateral fornix vary, as in Liu, Gross, Wheatley, Concha, and Beaulieu (2013), who, after studying Wallerian degeneration in the fornix in unilateral TLE patients pre- and post-surgery, found little change in the contralateral fornix in five out of six subjects.

The WM abnormalities in commissural pathways found in this study give support to their role in contralateral seizure propagation. However, the presence of diffuse FA reduction, increased MD and WM volume decrease in other projection or association WM tracts when compared to healthy controls and to TLE+UHS patients, provide evidence of seizure transmission through indirect circuits such as the frontal lobe (orbitofrontal, cingulate) and subcortical routes (the projection fibers of the fornix connecting the hippocampus with septal nuclei and mammillary bodies and their

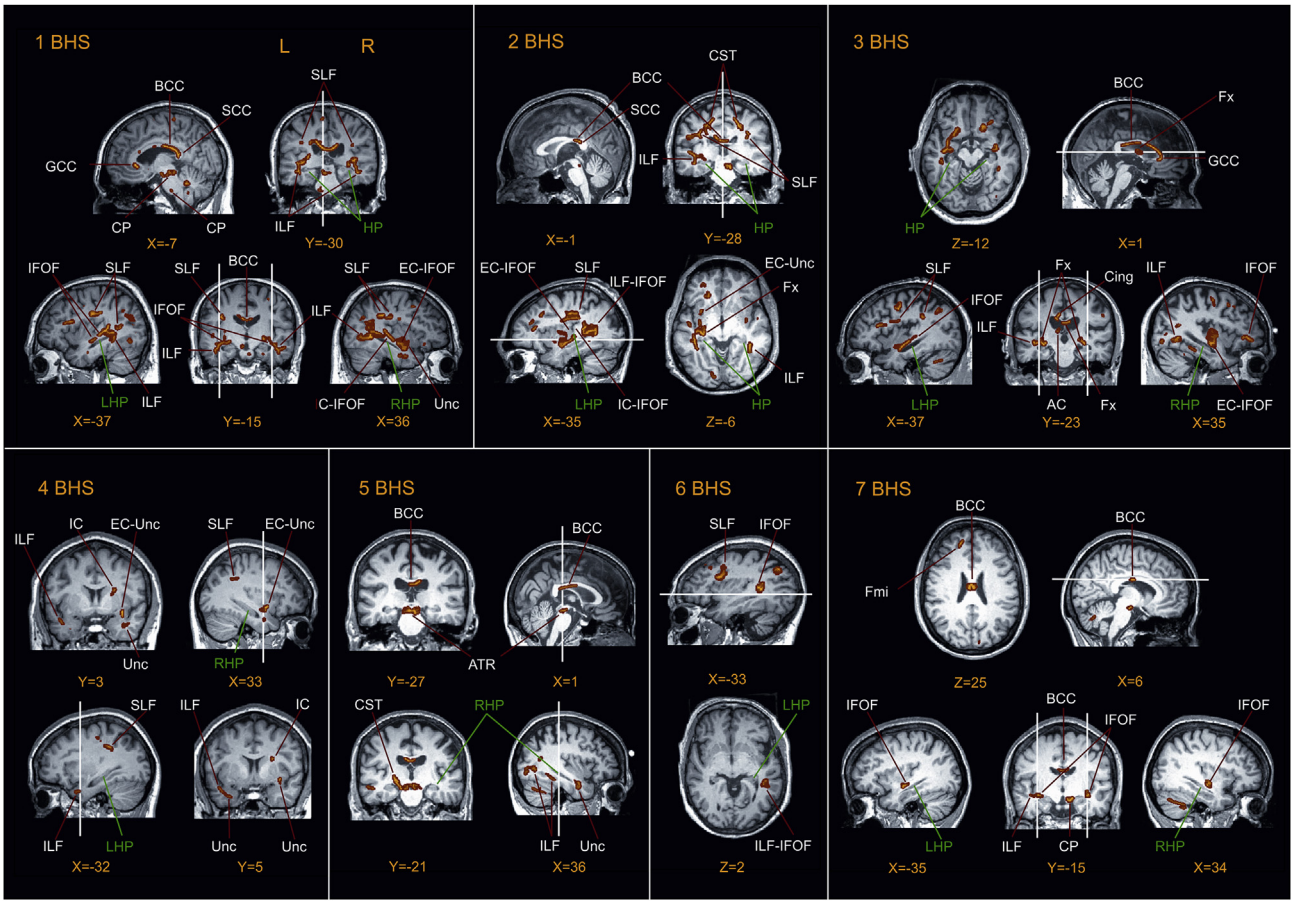


**Fig. 3 – Single patient TBSS analysis: regions with decreased FA in each TLE+BHS patient (separately) as compared with control subjects. In yellow-red, areas in which each patient has lower FA than the control group ($p < .05$, using Crawford's t-test) are depicted. ATR: anterior thalamic radiation; BCC: body of corpus callosum; CP: cerebellar peduncle; CST: corticospinal tract; EC: external capsule; Fmi: forceps minor; Fx: fornix; GCC: genu corpus callosum; HP: hippocampus; IC: internal capsule; IFOF: inferior fronto-occipital fasciculus; ILF: inferior longitudinal fasciculus; LHP: left hippocampus; SCC: splenium corpus callosum; SLF: superior longitudinal fasciculus; RHP: right hippocampus; Unc: uncinate. L: left hemisphere; R: right hemisphere.**

projections to the anterior and midline thalamic nuclei and the midbrain reticular formation and their return projections to mesial temporal structures) (Adam, 2006; Bertashius, 1991; Gloor et al., 1993; Lieb et al., 1987; Wada, 1991).

It is conceivable that the abnormal WM volume and DTI values observed here may be related to damage of the axonal pathways involved in seizure ictal spread or to secondary WM loss in connected areas (Diehl et al., 2008). Furthermore, synaptic alterations have been observed during the process of secondary epileptogenesis (Khalilov, Holmes, & Ben-Ari, 2003), suggesting that anatomically distant areas undergo a physiological change consequent to neuronal alterations in the primary epileptogenic zone (Morrell, 1989). Different mechanisms have been suggested as altering FA/MD DTI values: intracellular and extracellular fluid exchange, blood–brain barrier damage, neuronal cell death and axonal demyelination (Seidenberg et al., 2005; Song et al., 2003). The few histological studies examining the relationship between recurrent seizures and extrahippocampal remote damage (Concha et al., 2010; Ozdogmus et al., 2009; Van Eijsden et al., 2011), supported by the findings from in vivo hippocampal studies, show that axonal demyelination, formation of axonal spines, increase in interstitial fluid volume due to edema, replacement of axons with glial cells and astrocyte proliferation may all be associated with the damage caused by seizure activity and seizure-induced cell death (Freidman, Kaufer, & Heinemann, 2009; Sutula, 2001; Sutula, Hagen, & Pitkanen, 2003). Therefore, the overall pattern of WM volume and FA/MD changes seen in this study is consistent with the direct effect of axonal damage and associated secondary Wallerian degeneration, possibly due to cell loss, caused by repetitive seizure spread and interictal spikes propagating through WM portions of the epileptic network (Otte, Dijkhuizen, et al., 2012; Otte, Van Eijsden, et al., 2012). Moreover, the systemic effects of seizures such as hypoxia and vasoconstriction, antiepileptic drug treatment, altered brain development and plasticity-related reorganization of local and global WM networks may also contribute to these diffuse WM abnormalities

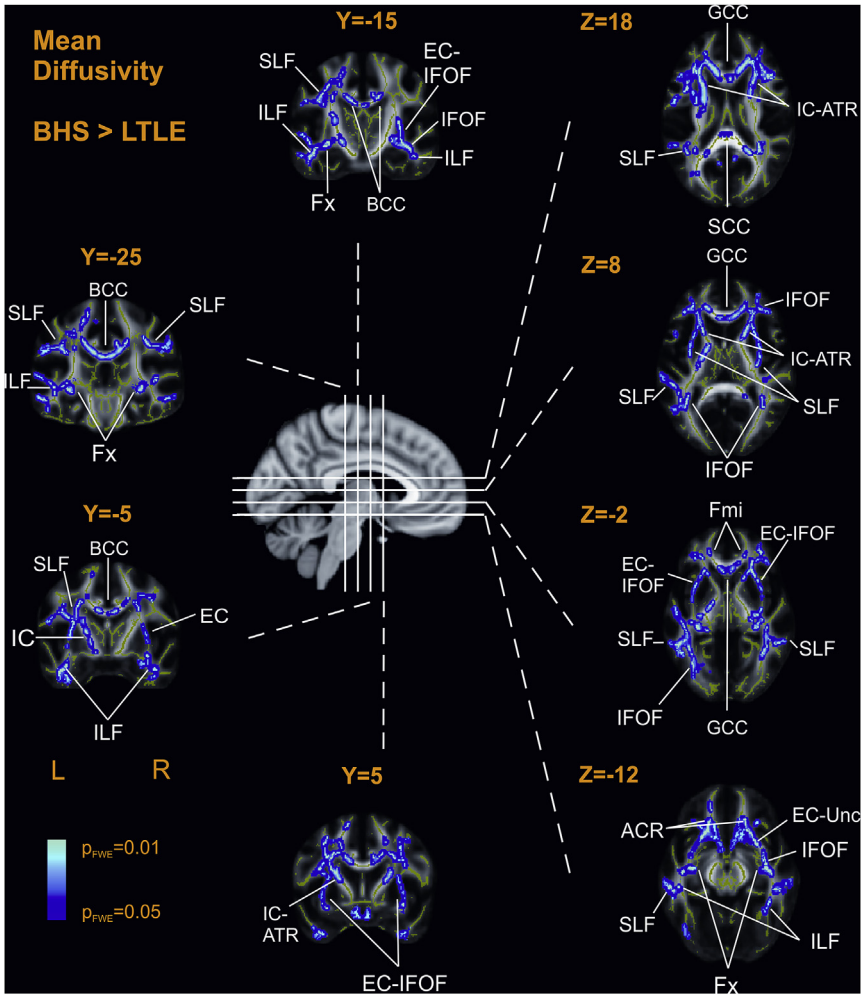


**Fig. 4 – Significant clusters of increased MD in TLE+BHS patients found with TBSS analysis when compared with unilateral TLE patients. Results are shown at a FWE-corrected $p < .05$ threshold. Significant clusters representing increases in MD in TLE+BHS patients compared with the TLE+UHS group are shown in light to dark blue. All clusters are projected onto a Montreal Neurological Institute FA template (FMRIB58_FA, MNI152 space) provided by FSL, and the mean group FA skeleton is shown in green. ACR: anterior corona radiate; ATR: anterior thalamic radiation; BCC: body of corpus callosum; Cing: cingulum; EC: external capsule; Fmi: forceps minor; Fx: fornix; IC: internal capsule; GCC: genu corpus callosum; IFOF: inferior fronto-occipital fasciculus; ILF: inferior longitudinal fasciculus; SCC: splenium corpus callosum; SLF: superior longitudinal fasciculus; Unc: uncinate. L: left hemisphere; R: right hemisphere.**

(Chen et al., 2013; Günbey et al., 2011; Zhao, Ma, Suh, & Schwartz, 2009).

Another interesting finding of the present study, provided by this particular cohort of patients with TLE+BHS, was that although all patients have bilateral video-EEG disturbance and bilateral MRI-confirmed HS, our multimodal analysis showed more severe damage in the left rather than the right hemisphere, even when compared to the left unilateral TLE with HS sample (see Tables 4–6). It is widely accepted that patients with left TLE generally show greater impairment in learning and memory than those with right temporal lobe epilepsy both before and after surgical treatment (Bell & Davies, 1998; Helmstaedter & Elger, 2009). There is also growing evidence to suggest that patients with left TLE show a more distributed, bilateral pattern of structural changes compared to those with right TLE (Bonilha et al., 2007; Coan, Appenzeller, Bonilha, Li, & Cendes, 2009; Keller & Roberts, 2008; Miró et al., 2014; Riederer et al., 2008). It is known that the left hemisphere not only matures later and to a larger extent than the right hemisphere, but it also undergoes a more prolonged maturation (Corballis & Morgan, 1978; Pujol et al., 2006). Therefore, it may be more vulnerable (particularly WM) to early brain insults like seizures. Moreover, due to perinatal vascular asymmetry in the hemispheres, the left hemisphere is known to be more vulnerable to hypoxic-ischemic insult (Mullart et al., 1995; Njiokiktjien, 2006) which has devastating effects on the hippocampus and surrounding regions (Schmidt-Kastner & Freund, 1991). However, none of these factors would clearly

**Table 6 – TBSS analysis: representative pathways in the whole-brain analysis for the MD maps for TLE+BHS > TLE+UHS contrast (tracts showing higher MD in TLE+BHS patients than in TLE+UHS patients), with their respective *p*-values ($p < .05$ Family Wise Error-corrected) and MNI coordinates.**

| White Matter tract | Hemisphere | *p* value | Peak MNI coordinates | | |
|---|---|---|---|---|---|
| | | | x | y | z |
| BCC | L | .008 | −14 | 18 | 25 |
| GCC-Fmi | L | .009 | −12 | 28 | 16 |
| ACR-ATR | L | .009 | −24 | 11 | 18 |
| ACR-IFOF | L | .009 | −23 | 29 | 5 |
| IC | L | .010 | −18 | −5 | 9 |
| SLF | L | .011 | −38 | −19 | 31 |
| ATR-IC | R | .012 | 21 | 20 | 3 |
| Unc | R | .014 | 22 | 21 | −10 |
| ACR | R | .014 | 26 | 29 | 5 |
| EC | R | .014 | 27 | 18 | 7 |
| GCC-Fmi | R | .015 | 11 | 28 | 13 |
| IFOF | R | .016 | 33 | 37 | 5 |
| EC-Unc | L | .016 | −23 | 16 | −12 |
| Fx | R | .016 | 33 | −18 | −9 |
| ILF | L | .017 | −34 | −66 | −2 |
| IFOF-EC | R | .019 | 34 | 7 | −5 |
| BCC | R | .020 | 11 | 17 | 24 |
| Cing | R | .020 | 9 | 18 | 28 |
| Cing | L | .024 | −10 | −38 | 31 |
| Fx | L | .028 | −29 | −20 | −7 |
| Unc | L | .028 | −33 | 1 | −9 |
| SCC | L | .037 | −6 | −33 | 20 |
| SCC | R | .039 | 4 | −32 | 20 |
| SLF | R | .047 | 36 | −25 | 35 |
| ILF | R | .047 | 37 | −52 | −3 |

Coordinates are given following the Montreal Neurologic Institute system. WM: white matter; ACR: anterior corona radiata; ATR: anterior thalamic radiation; BCC: body of corpus callosum; Cing: cingulum; EC: external Capsule; Fmi: forceps minor; Fx: fornix; GCC: genu corpus callosum; IC: internal capsule; IFOF: inferior fronto-occipital fasciculus; ILF: inferior longitudinal fasciculus; SCC: splenium corpus callosum; SCP: superior cerebellar peduncle; SCR: superior corona radiata; SLF: superior longitudinal fasciculus; Unc: uncinate. L, left hemisphere; R, right hemisphere.

explain why in our cohort of TLE+BHS patients, larger differences were observed in the left hemisphere, even when compared with unilateral TLE patients with left HS. Another compelling theory that might explain the greater impairment of left hemisphere GM and WM in this sample is related to the increased WM connectivity between the left hemisphere and the rest of the brain. This increased connectivity is probably associated with language dominance and is therefore particularly relevant for the frontal and temporal regions including the hippocampus (Glauske, Schlote, Bratzke, & Singer, 2000; Good et al., 2001; Powell et al., 2006; Pujol et al., 2002). This increased structural connectivity could induce more excitotoxic damage to both the left-hemisphere neocortex and WM tissue when propagating repetitive seizures, or to more neuronal loss from deafferentation secondary to hippocampal atrophy on the left hemisphere (Bonilha et al., 2007; Coan et al., 2009; Muller et al., 2006).

One of the possible caveats of our study comes from the fact that one the TLE+BHS patients (TLE+BHS 6) had a major depressive syndrome and was under anti-depressant treatment. In patients with major depressive disorder, impaired WM integrity is not an uncommon finding. Indeed, the meta-analyses of Liao et al. (2013) evidenced 4 main locations of abnormal WM in major depression studies: right and left frontal lobe and right fusiform gyrus and occipital lobe with involvement of the right inferior longitudinal fasciculus (ILF); right inferior fronto-occipital fasciculus (IFOF); right posterior thalamic radiation and interhemispheric fibers running through the genu; and the body of the corpus callosum. However, even though there are common WM disrupted pathways between TLE and major depression, the fact that there was only one patient with major depression in the TLE+BHS group and the results from the single-patient analysis make it unlikely that the present findings might be solely driven influenced by the comorbidity of patient number 6. Indeed, although our study included a small sample size, which could be considered an important limitation, the aforementioned single-patient analysis (in which we compared each patient's FA map to the control group, see Gillebert, Humphreys, & Mantini, 2014 and Tuomiranta et al., 2014 for similar recent applications) revealed FA decreases in all patients, including patient 6. Hence, the use of non-invasive MRI analysis techniques, such as those used in the present study applied to individual cases, could also help to delineate the extent of structural abnormalities in particular patients. In addition, it is important to consider that TBSS and VBM were consistent in detecting WM derangement in several areas. This information could have a particularly important role in the assessment of disease severity, tracking of disease progression and prognosis assessment, therapy monitoring (intracranial EEG planning) and optimization of presurgical tissue resection planning in patients with epilepsy. Network changes may become a promising additional form of disease quantification of unilateral and bilateral temporal lobe epilepsy and other forms of epilepsy.

In summary, the current results support the idea that commissural pathways (especially the corpus callosum but also the anterior and hippocampal commissure) play a contributory role together with the indirect circuits (such as the orbitofrontal, cingulate and subcortical routes) in inter-hemispheric TLE seizure propagation. Moreover, this type of connectivity analysis offers important new perspectives and insights into the nature of epilepsy, such as the characterization of seizure propagation patterns. It could also play a particularly compelling role in the assessment of disease severity and in tracking progression or presurgical planning in patients with epilepsy.

## Acknowledgments

This project was supported by the Spanish Government (Ministerio de Ciencia e Innovación, PSI2011-29219, awarded to ARF). Júlia Miró is a recipient of a Rio Hortega research contract (code: CM10/00077) from the Carlos III National Health Institute (Spanish Government).

## Supplementary data

Supplementary data related to this article can be found at http://dx.doi.org/10.1016/j.cortex.2015.03.018.

## REFERENCES


Adam, C. (2006). How do the temporal lobes communicate in medial temporal lobe seizures? *Revue Neurologique, 162*(8–9), 813–818.

Adam, C., Hasboun, D., Clemenceau, S., Dupont, S., Baulac, M., & Hazemann, P. (2004). Fast contralateral propagation of after-discharges induced by stimulation of medial temporal lobe. *Journal of Clinical Neurophysiology, 21*, 399–403.

Afzali, M., Sotlanian-Zadeh, H., & Elisevich, K. V. (2011). Tract based spatial statistical analysis and voxel based morphometry of diffusion indices in temporal lobe epilepsy. *Computers in Biology and Medicine, 41*(12), 1082–1091.

Aggleton, J. P., Desimoner, R., & Mishkin, M. (1986). The origin, course, and termination of the hippocampothalamic projections in the macaque. *Journal of Comparative Neurology, 243*, 409–421.

Aggleton, J. P., Friedman, D. P., & Mishkin, M. (1987). A comparison between the connections of the amygdala and hippocampus with the basal forebrain in the macaque. *Experimental Brain Research, 67*, 556–568.

Andersson, J. L. R., Jenkinson, M., & Smith, S. (2007a). *Non-linear optimisation. FMRIB technical report TR07JA1*.

Andersson, J. L. R., Jenkinson, M., & Smith, S. (2007b). *Non-linear registration, aka spatial normalization. FMRIB technical report TR07JA2*.

Arfanakis, K., Hermann, B. P., Rogers, B. P., Carew, J. D., Seidenberg, M., & Meyerand, M. E. (2002). Diffusion tensor MRI in temporal lobe epilepsy. *Magnetic Resonance in Imaging, 20*, 511–519.

Asady-Pooya, A. A., Sharan, A., Nei, M., & Sperlin, M. R. (2008). Corpus callosotmy. *Epilepsy and Behavior, 13*(2), 271–278.

Ashburner, J. (2007). A fast diffeomorphic image registration algorithm. *NeuroImage, 38*(1), 95–113.

Ashburner, J., & Friston, K. J. (2000). Voxel-based morphometry–the methods. *NeuroImage, 11*(6 Pt1), 805–821.

Ashburner, J., & Friston, K. J. (2005). Unified segmentation. *NeuroImage, 26*(3), 839–851.

Ashburner, J., & Friston, K. J. (2009). Computing average shaped tissue probability templates. *NeuroImage, 45*(2), 333–341.

Beaulieu, C. (2002). The basis of anisotropic water diffusion in the nervous system. *NMR in Biomedicine, 15*(7–8), 435–455.

Bell, B. D., & Davies, K. G. (1998). Anterior temporal lobectomy, hippocampal sclerosis, and memory: recent neuropsychological findings. *Neuropsychology Review, 8*, 25–41.

Bertashius, K. M. (1991). Propagation of human complex-partial seizures: a correlation analysis. *Electroencephalography and Clinical Neurophysiology, 78*(5), 333–340.

Bettus, G., Guedj, E., Joyeux, F., Confrot-Gouny, S., Soulier, E., Laguitton, V., et al. (2009). Decreased basal fMRI functional connectivity in epileptogenic networks and contralateral compensatory mechanisms. *Human Brain Mapping, 30*(5), 1580–1591.

Bonilha, L., Edwards, J. C., Kinsman, S. L., Morgan, P. S., Fridriksson, J., Rorden, C., et al. (2010). Extrahippocampal gray matter loss and hippocampal deafferentation in patients with temporal lobe epilepsy. *Epilepsia, 51*, 519–528.

Bonilha, L., Rorden, C., Halford, J. J., Eckert, M., Appenzeller, S., Cendes, F., et al. (2007). Asymmetrical extra-hippocampal grey matter loss related to hippocampal atrophy in patients with medial temporal lobe epilepsy. *Journal of Neurology Neurosurgery & Psychiatry, 78*, 286–294.

Cámara, E., Rodríguez-Fornells, A., & Münte, T. F. (2010). Microstructural brain differences predict functional hemodynamic responses in a reward processing task. *Journal of Neuroscience, 30*(34), 11398–11402.

Catani, M., Allin, M. P., Husain, M., Pugliese, L., Mesulam, M. M., Murray, R. M., et al. (2007). Symmetries in human brain language pathways correlate with verbal recall. *Proceedings of the National Academy of Sciences of the United States of America, 104*(43), 17163–17168.

Catani, M., & Thiebaut de Schotten, M. (2012). *Atlas of human brain connections*. New York: Oxford university press.

Cendes, F. (2005). Progressive hippocampal and extrahippocampal atrophy in drug resistant epilepsy. *Current Opinion In Neurology, 18*(2), 173–177.

Cendes, F., Li, L. M., Watson, C., Andermann, F., Dubeau, F., & Arnold, D. L. (2000). Is ictal recording mandatory in temporal lobe epilepsy? Not when the interictal electroencephalogram and hippocampal atrophy coincide. *Archives of Neurology, 57*(4), 497–500.

Chen, Y. H., Kuo, T. T., Chu, M. T., Ma, H. I., Chiang, Y. H., & Huang, E. Y. (2013). Postnatal systemic inflammation exacerbates impairment of hippocampal synaptic plasticity in an animal seizure model. *Neuroimmunomodulation, 20*(4), 223–232.

Coan, A. C., Appenzeller, S., Bonilha, L., Li, L. M., & Cendes, F. (2009). Seizure frequency and lateralization affect progression of atrophy in temporal lobe epilepsy. *Neurology, 73*, 834–842.

Concha, L. (2013). A macroscopic view of microstructure: using diffusion-weighted images to infer damage, repair, and plasticity of white matter. *Neuroscience, 17*. S0306–4522(13) 0074-4.

Concha, L., Beaulieu, C., Collins, D. L., & Gross, D. W. (2009). White-matter diffusion abnormalities in temporal-lobe epilepsy with and without mesial temporal sclerosis. *Journal of Neurology Neurosurgery & Psychiatry, 80*, 312–319.

Concha, L., Beaulieu, C., & Gross, D. W. (2005). Bilateral limbic diffusion abnormalities in unilateral temporal lobe epilepsy. *Annals of Neurology, 57*(2), 188–196.

Concha, L., Livy, D. J., Beaulieu, C., Whatley, B. M., & Gross, D. W. (2010). In vivo diffusion tensor imaging and histopathology of the fimbria-fronix in temporal lobe epilepsy. *Journal of Neuroscience, 30*(3), 996–1002.

Corballis, M. C., & Morgan, M. (1978). On the biological basis of human laterality: I. Evidence for a maturational left-right gradient. *Behavioral and Brain Sciences, 2*, 261–269.

Crawford, J. R., & Garthwaite, P. H. (2004). Statistical methods for single-case studies in neuropsychology: comparing the slope of a patient's regression line with those of a control sample. *Cortex, 40*(3), 533–548.

Crawford, J. R., & Howell, D. C. (1998). Regression equations in clinical neuropsychology: an evaluation of statistical methods for comparing predicted and obtained scores. *Journal of Clinical and Experimental Neuropsychology, 20*(5), 755–762.

Di Virgilio, G., Clarke, S., Pizzolato, G., & Schaffner, T. (1999). Cortical regions contributing to the anterior commissure in man. *Experimental Brain Research, 124*, 1–7.

Diehl, B., Busch, R. M., Duncan, J. S., Piao, Z., Tkach, J., & Luders, H. O. (2008). Abnormalities in diffusion tensor imaging of the uncinate fasciculus relate to reduced memory in temporal lobe epilepsy. *Epilepsia, 49*(8), 1409–1418.

Engel, J., Jr. (1996). Introduction to temporal lobe epilepsy. *Epilepsy Research, 26*, 141–150.

Freidman, A., Kaufer, D., & Heinemann, U. (2009). Blood-brain barrier breakdown-inducing astrocytic transformation: novel

targets for the prevention of epilepsy. *Epilepsy Research, 85*(2–3), 142–149.
Gillebert, C. R., Humphreys, G. W., & Mantini, D. (2014). Automated delineation of stroke lesions using brain CT images. *NeuroImage: Clinical, 4*, 540–548.
Glauske, R. E., Schlote, W., Bratzke, H., & Singer, W. (2000). Interhemispheric asymmetries of the modular structure in human temporal cortex. *Science, 289*(5486), 1946–1949.
Gloor, P., Salanova, V., Olivier, A., & Quesney, L. F. (1993). The human dorsal hippocampal commissure. *Brain, 116*, 1249–1273.
Good, C. D., Johnsrude, I., Ashburner, J., Henson, R. N., Friston, K. J., & Frackowiak, R. S. (2001). Cerebral asymmetry and the effects of sex and handedness on brain structure: a voxel-based morphometric analysis of 465 normal adult human brains. *NeuroImage, 14*(3), 685–700.
Gross, D. W. (2011). Diffusion tensor imaging in temporal lobe epilepsy. *Epilepsia, 52*(Suppl. 4), 32–34.
Gross, D. W., Concha, L., & Beaulieu, C. (2006). Extratemporal white matter abnormlities in mesial temporal lobe epilepsy demonstrated with diffusion tensor imaging. *Epilepsia, 47*(8), 1360–1363.
Günbey, H. P., Ercan, K., Findikoglu, A. S., Bilir, E., Karaoglanoglu, M., Komurcu, F., et al. (2011). Secondary corpus callosum abnormalities associated with antiepileptic drugs in temporal lobe epilepsy. A diffusion tensor imaging study. *Neuroradiology Journal, 24*(2), 316–323.
Helmstaedter, C., & Elger, C. E. (2009). Chronic temporal lobe epilepsy: a neurodevelopmental or progressively dementing disease? *Brain, 132*, 2822–2830.
Hoppe, C., Elger, C. E., & Helmstaedter, C. (2007). Long-term memory impairment in patients with focal epilepsy. *Epilepsia, 48*(Suppl. 9), 26–29.
Jackson, G. D., Berkovic, S. F., Tress, B. M., Kalnins, R. M., Fabinyi, G. C., & Bladin, P. F. (1990). Hippocampal sclerosis can be reliably detected by magnetic resonance imaging. *Neurology, 40*, 1869–1875.
Kaplan, E., Goodglass, H., & Weintraub, S. (1983). *Boston naming test*. Philadelphia: Lea & Febiger.
Keller, S. S., & Roberts, N. (2008). Voxel-based morphometry of temporal lobe epilepsy: an introduction and review of the literature. *Epilepsia, 49*, 741–757.
Keller, S. S., Schoene-Bake, J. C., Gerdes, J. S., Weber, B., & Deppe, M. (2012). Concomitant fractional anisotropy and volumetric abnormalities in temporal lobe epilepsy: cross-sectional evidence for progressive neurologic injury. *PLoS One, 7*(10), e46791.
Khalilov, I., Holmes, G. L., & Ben-Ari, Y. (2003). In vitro formation of a secondary epileptogenic mirror focus by interhippocampal propagation of seizures. *Nature Neuroscience, 6*, 1079–1085.
Knake, S., Salat, dh, Halgren, E., Halko, M. A., Greve, D. N., & Grant, P. E. (2009). Changes in white matter microstructure in patients with TLE and hippocampal sclerosis. *Epiletic Disorders, 11*(3), 244–250.
Kuzniecky, R., Bilir, E., Gilliam, F., Faught, E., Martin, R., & Hugg, J. (1999). Quantitative MRI in temporal lobe epilepsy: evidence for fornix atrophy. *Neurology, 53*, 496–501.
Liao, Y., Huang, X., Wu, Q., Yang, C., Kuang, W., Du, M., et al. (2013). Is depression a disconnection syndrome? Meta-analysis of diffusion tensor imaging studies in patients with MDD. *Journal of Psychiatry & Neuroscience, 38*(1), 49–56.
Lieb, J. P., Hoque, K., Skomer, E. C., & Song, X. W. (1987). Inter-hemispheric propagation of human mesial temporal lobe seizures: a coherence/phase analysis. *Electroencephalography and Clinical Neurophysiology, 67*(2), 101–119.
Liu, M., Gross, D. W., Wheatley, B. M., Concha, L., & Beaulieu, C. (2013). The acute phase of Wallerian degenearation: longitudinal diffusion tensor imaging of the fornix following temporal lobe surgery. *NeuroImage, 74*, 128–139.
López-Barroso, D., Catani, M., Ripollés, P., Dell'Acqua, F., Rodríguez-Fornells, A., & de Diego Balaguer, R. (2013). Word learning is mediated by the left arcuate fasciculus. *Proceedings of the National Academy of Sciences of the United States of America, 110*(32), 13168–13173.
Malmgren, K., & Thom, M. (2012). Hippocampal sclerosis- origins and imaging. *Epilepsia, 53*(Suppl. 4), 19–33.
Marques, C. M., Caboclo, L. O., da Silva, T. I., Noffs, M. H., Carrete, H., Jr., Lin, K., et al. (2007). Cognitive decline in temporal lobe epilepsy due to unilateral hippocampal sclerosis. *Epilepsy and Behaviour, 10*, 477–485.
Mechelli, A., Price, C. J., Friston, K. J., & Ashburner, J. (2005). Voxel-based morphometry of the human brain: methods and applications. *Current Medical Imaging Reviews, 1*, 105–113.
Milner, B. (1980). Complementary functional specializations of the human cerebral hemispheres. In R. Levi-Montalcini (Ed.), *Nerve cells, transmitters and behaviour* (pp. 601–625). Amsterdam: Elsevier/North-Holland.
Miró, J., Ripollés, P., López-Barroso, D., Vilà-Balló, A., Juncadella, M., de Diego-Balaguer, R., et al. (2014). Atypical language organization in temporal lobe epilepsy revealed by a passive semantic paradigm. *BMC Neurology, 14*(1), 98.
Mori, S., Faria, A. V., Oishi, K., & van Zijl, P. C. M. (2005). *MRI atlas of human white matter*. Amsterdam, The Netherlands: Elsevier.
Morrell, F. (1989). Varieties of human secondary epileptogenesis. *Journal of Clinical Neurophysiology, 6*, 227–275.
Mullaart, R. A., Daniels, O., Hopman, J. C., de Haan, A. F., Stoelinga, G. B., & Rotteveel, J. J. (1995). Asymmetry of the cerebral blood flow: an ultrasound Doppler study in preterm newborns. *Pediatric Neurology, 13*, 319–322.
Muller, S. G., Laxer, K. D., Cashdollar, N., Buckley, S., Paul, C., & Weiner, M. W. (2006). Voxel-based optimized morphometry (VBM) of gray and white matter in temporal lobe epilepsy (TLE) with and without mesial temporal sclerosis. *Epilepsia, 47*, 900–907.
Napolitano, C. E., & Orriols, M. A. (2010). Graduated and sequential propagation in mesial temporal epilepsy: analysis with scalp ictal EEG. *Journal of Clinical Neurophysiology, 27*(4), 285–291.
Nichols, T. E., & Holmes, A. P. (2002). Nonparametric permutation tests for functional neuroimaging: a primer with examples. *Human Brain Mapping, 15*, 1–25.
Njiokiktjien, C. (2006). Differences in vulnerability between the hemispheres in early childhood and adulthood. *Fiziol Cheloveka, 32*, 45–50.
Oldfield, R. C. (1971). The assessment and analysis of handedness: the Edinburgh inventory. *Neuropsychologia, 9*, 97–113.
Otte, W. M., Dijkhuizen, R. M., van Meer, M. P., van der Hel, W. S., Verlinde, S. A., van Nieuwenhuizen, O., et al. (2012a). Characterization of functional and structural integrity in experimental focal epilepsy: reduced network efficiency coincides with white matter changes. *PLoS One, 7*(7), e39078.
Otte, W. M., Van Eijsden, P., Sander, J. W., Duncan, J. S., Djikhuizen, R. M., & Braun, K. P. (2012b). A meta-analysis of white matter changes in temporal lobe epilepsy as studied with diffusion tensor imaging. *Epilepsia, 53*(4), 659–667.
Ozdogmus, O., Cavdar, S., Ersoy, Y., Ercan, F., & Uzun, I. (2009). A preliminary study, using electron and light-microscopic methods, of axon numbers in the fornix in autopsies of patients with temporal lobe epilepsy. *Anatomical Science International, 84*(1–2), 2–6.
Peña-Casanova, J. (2005). *Integrated neuropsychological exploration program – Barcelona test revised*. Barcelona: Masson.
Powell, H. W., Parker, G. J., Alexander, D. C., Symms, M. R., Boulby, P. A., Wheeler-Kingshott, C. A., et al. (2006).

Hemispheric asymmetries in language-related pathways: a combined functional MRI and tractography study. *NeuroImage, 32*(1), 388–399.
Pujol, J., López-Sala, A., Deus, J., Cardoner, N., Sebastián-Gallés, N., Conesa, G., et al. (2002). The lateral asymmetry of the human brain studied by volumetric magnetic resonance imaging. *NeuroImage, 17*(2), 670–679.
Pujol, J., Soriano-Mas, C., Ortiz, H., Sebastian-Galles, N., Losilla, J. M., & Deus, J. (2006). Myelination of language-related areas in the developing brain. *Neurology, 66*, 339–343.
Reitan, R. M. (1992). *Trail Making Test: Manual for administration and scoring*. Tucson: Reitan Neuropsychology Laboratory.
Riederer, F., Lanzenberger, R., Kaya, M., Prayer, D., Serles, W., & Baumgartner, C. (2008). Network atrophy in temporal lobe epilepsy: a voxel-based morphometry study. *Neurology, 71*, 419–425.
Ripollés, P., Marco-Pallarés, J., de Diego-Balaguer, R., Miró, J., Falip, M., Juncadella, M., et al. (2012). Analysis of automated methods for spatial normalization of lesioned brains. *NeuroImage, 60*(2), 1296–1306.
Schmidt-Kastner, R., & Freund, T. F. (1991). Selective vulnerability of the hippocampus in brain ischemia. *Neuroscience, 40*, 599–636.
Seidenberg, M., Kelly, K. G., Parrish, J., Geary, E., Dow, C., Rutecki, P., et al. (2005). Ipsilateral and contralateral MRI volumetric abnormalities in chronic unilateral temporal lobe epilepsy and their clinical correlates. *Epilepsia, 46*, 420–430.
Smith, S. M., Jenkinson, M., Johansen-Berg, H., Rueckert, D., Nichols, T. E., Mackay, C. E., et al. (2006). Tract-based spatial statistics: voxelwise analysis of multi-subject diffusion data. *NeuroImage, 31*(4), 1487–1505.
Smith, S. M., Jenkinson, M., Woolrich, M. W., Beckmann, C. F., Behrens, T. E., Johansen Berg, H., et al. (2004). Advances in functional and structural MR image analysis and implementation as FSL. *NeuroImage, 23*(Suppl. 1), S208–S219.
Smith, S. M., & Nichols, T. E. (2009). Threshold-free cluster enhancement: addressing problems of smoothing, threshold dependence and localisation in cluster inference. *NeuroImage, 44*(1), 83–98.
Smith, S. M., Zhang, Y., Jenkinson, M., Chen, J., Matthews, P. M., Federico, A., et al. (2002). Accurate, robust, and automated longitudinal and cross-sectional brain change analysis. *NeuroImage, 17*(1), 479–489.
So, N., Olivier, A., Andermann, F., Gloor, P., & Quesney, L. F. (1989). Results of surgical treatment in patients with bitemporal epileptiform abnormalities. *Annals of Neurology, 25*(5), 432–439.
Song, S. K., Sun, S. W., Ju, W. K., Lin, S. J., Cross, A. H., & Neufeld, A. H. (2003). Diffusion tensor imaging detects and differentiates axon and myelin degeneration in mouse optic nerve after retinal ischemia. *NeuroImage, 20*, 1714–1722.
Song, S. K., Sun, S. W., Ramsbottom, M. J., Chang, C., Russell, J., & Cross, A. H. (2002). Dysmyelination revealed through MRI as increased radial (but unchanged axial) diffusion of water. *NeuroImage, 17*(3), 1429–1436.
Spencer, S. S., Marks, D., Katz, A., Kim, J., & Spencer, D. D. (1992). Anatomic correlates of interhippocampal seizure propagation time. *Epilepsia, 33*, 862–873.
Supcun, B., Khaleghi, G., Zeraati, M., Stummer, W., Speckmann, E. J., & Gorji, A. (2012). The effects of titanic stimulation on plasticity of remote synapses in the hippocampus-perirhinal cortex-amygdala Network. *Synapse, 66*, 965–974.
Sutula, T. (2001). Secondary epileptogenesis, kindling, and intractable epilepsy: a reappraisal from the perspective of neural plasticity. In J. J. Engel, P. Schwartzkroin, S. Moshe, & D. Lowenstein (Eds.), *Brain plasticity epilepsy* (Vol. 45, pp. 355–379). Academic Press.
Sutula, T. P. (2004). Mechanisms of epilepsy progression: current theories and perspectives from neuroplasticity in adulthood and development. *Epilepsy Research, 60*, 161–171.
Sutula, T. P., Hagen, J., & Pitkanen, A. (2003). Do epileptic seizures damage the brain? *Current Opinion In Neurology, 16*, 189–195.
Tatum, W. O., 4th (2012). Mesial temporal lobe epilepsy. *Journal of Clinical Neurophysiology, 29*(5), 356–365.
Towgood, K. J., Meuwese, J. D. I., Gilbert, S. J., Turner, M. S., & Burgess, P. W. (2009). Advantages of the multiple case series approach to the study of cognitive deficits in autism spectrum disorder. *Neuropsychologia, 47*(13), 2981–2988.
Tuomiranta, L., Càmara, E., Froudist, W. S., Ripollés, P., Saunavaara, J. P., Parkkola, R., et al. (2014). Hidden word learning capacity in aphasia. *Cortex, 50*, 174–191.
Van Eijsden, P., Otte, W. M., van der Hel, W. S., van Nieuwenhuizen, O., Dijkhuizen, R. M., de Graaf, R. A., et al. (2011). In vivo diffusion tensor imaging and ex vivo histologic characterization of white matter pathology in post-status epilepticus model of temporal lobe epilepsy. *Epilepsia, 52*, 841–845.
Voets, N. L., Beckmann, C. F., Cole, D. M., Hong, S., Bernasconi, A., & Bernasconi, N. (2012). Structural substrates for resting network disruption in temporal lobe epilepsy. *Brain, 135*(Pt 8), 2350–2357.
Wada, J. A. (1991). Transhemispheric horizontal channels for transmission of epileptic information. *Japanese Journal of Psychiatry and Neurology, 45*(2), 235–242.
Wada, J. A. (1995). Midline subcortical structures for transhemispheric ictal and interictal transmission. In A. G. Reeves, & D. W. Roberts (Eds.), *Advances in behavioral biology: Vol. 45. Epilepsy and the corpus callosum 2* (pp. 61–78). New York: Plenum.
Wechsler, D. (1997). *Wechsler adult intelligence scale – Third Edition (WAIS-III): Administration and scoring manual*. San Antonio, TX, USA: The Psychological Corp.
Wechsler, D. (2004). *WMS III. Escala de memoria de Wechsler-III*. Madrid: TEA.
Woermann, F. G., Barker, G. J., Birnie, K. D., Meencke, H. J., & Duncan, J. S. (1998). Regional changes in hippocampal T2 relaxation and volume: a quantitative magnetic resonance imaging study of hippocampal sclerosis. *Journal of Neurology Neurosurgery & Psychiatry, 65*, 656–664.
Woolrich, M. W., Jbadi, S., Patenaude, B., Chappell, M., Makni, S., Behrens, T., et al. (2009). Bayesian analysis of neuroimaging data in FSL. *NeuroImage, 45*(1 Suppl.), S173–S186.
Yogarajah, M., & Duncan, J. S. (2008). Diffusion-based magnetic resonance imaging and tractography in epilepsy. *Epilepsia, 49*(2), 189–200.
Zhao, M., Ma, H., Suh, M., & Schwartz, T. H. (2009). Spatiotemporal dynamics of perfusion and oximetry during ictal discharges in the rat neocortex. *Journal of Neuroscience, 29*(9), 2814–2823.